ORIGINAL RESEARCH PAPER

On tailored synthesis of nano CaCO$_3$ particles in a colloidal gas aphron system and evaluating their performance with response surface methodology for heavy metals removal from aqueous solutions

Hossein Mohammadifard, Mohammad C. Amiri*

Department of Chemical Engineering, Isfahan University of Technology, Isfahan, Iran

ABSTRACT

Heavy metals pollution in the environment is one of the serious problems in the field of water and wastewater management. In this study; calcium carbonate nanoparticles, synthesized by an efficient and novel method, were used as an adsorbent for the removal of lead and iron from aqueous solutions. To study the mechanism of adsorption, the kinetic and isotherm models were examined. The adsorption kinetics of process was found to follow a pseudo-second-order equation. The maximum monolayer adsorption capacities of calcium carbonate nanoparticles calculated from Langmuir isotherm were found to be 1210±30 mg/g for Pb(II) and 845±8 mg/g for Fe(II) ions, respectively. The response surface methodology based on three variable Box-Behnken design was utilized to evaluate the effects of temperature (25-65 ℃) and initial metal concentration (10-200 mg/L) on the sorption process. The optimum conditions for the removal process using calcium carbonate nanoparticles were found to be 200 mg/L at 25 ℃. Experimental data demonstrated that a precipitation transformation mechanism rather than adsorption enhances the removal efficiency.

Keywords: *Adsorption; Box-Behnken Design (BBD); Calcium Carbonate Nanoparticles; Pb(II) And Fe(II) Removal; Wastewater Treatment*

INTRODUCTION

Wastewater treatment has now become one of the most serious environmental challenges. Heavy metal pollutants are mostly exposed to the environment with the activities of various industries such as textile, mining, battery manufacturing, metal plating industries, etc [1]. Compared with other wastewaters, heavy metal-polluted waters are very dangerous since they directly expose human health to severe risks. The effects of lead on kidney, nervous system, reproductive system, liver, and brain [2]; mercury on the central nervous system, lung, and kidney [3]; cadmium on lung, kidney, liver, and reproductive organs [4]; and nickel on skin, lung, mucous membranes, and nervous system [5] are some of the associated health problems. Besides; unlike other contaminants, heavy metals cannot be processed by microorganisms and may accumulate in living organisms.

Faced with the mentioned problems, various physical and chemical methods; such as chemical precipitation, solvent extraction, ion exchange, coagulation and sedimentation flotation, membrane filtration, adsorption, and photoreduction have been applied for removing soluble metals from various aqueous solutions [6-12]. However, many of these techniques have some disadvantages. Low efficiency and production of a

* Corresponding Author Email: *amir33@cc.iut.ac.ir*

large amount of sludge in precipitation methods, requirements of expensive materials and high energy consumption in membrane methods are some of these limitations. In contrast, along with all these physicochemical methods; adsorption is recognized as an effective, low-cost, and easy to operate method [13]. Moreover; in some physical adsorption processes, the adsorbent can be regenerated and recycled by suitable desorption process. Development of cost-effective adsorbents with high efficiency has attracted a lot of interest in recent decades. The most current adsorbents for heavy metal removal can be categorized into activated carbon [14, 15], zeolites [16, 17], low-cost adsorbents (such as agricultural wastes and industrial byproducts) [18], and bioadsorbents [19].

Activated carbon (AC) adsorbents and zeolites have been widely used in adsorption processes; nevertheless, they are relatively expensive and sometimes have complicated synthesis methods. On the other hand, although bioadsorbents and low-cost adsorbents have partly reduced the cost of operation, but the removal capacity of these materials is quite low.

In recent years, nano-adsorbents have attracted a considerable attention because of their enhanced adsorption rate, capacity, and selectivity for heavy metals. Nanosized metal oxides, especially magnetic nanoparticles and their nanocomposites with organic compounds [20-22], and carbon nanotubes [2, 23] are the most studied nano-adsorbents. However, these adsorbents are usually had expensive synthesizing processes.

Calcium carbonate nanoparticles have shown a good capacity for the removal of heavy metals [24, 25]. Recently, a novel low-cost method for generation of calcium carbonate nanoparticles has been developed based on colloidal gas aphron (CGA) system [26]. In this experimental work, the prepared calcium carbonate nanoparticles generated in a CGA system were characterized and their applicability in lead and iron ions removal was investigated. Their adsorption kinetics and capacities in aqueous solutions for the undesirable ions were reported.

MATERIALS AND METHODS
Reagents

All the chemicals used in the study were of analytical grade and used as received without further purification. Calcium chloride dihydrate ($CaCl_2.2H_2O$), sodium carbonate (Na_2CO_3), lead(II) nitrate ($Pb(NO_3)_2$), and iron(II) sulfate heptahydrate ($FeSO_4.7H_2O$) were purchased from Merck. Hydrochloric acid (HCl) was obtained from Nirou Chlor Co. (Isfahan, Iran). Absolute ethanol (>99.5%) was obtained from Zanjan Co. (Zanjan, Iran). Sodium dodecyl sulfate (SDS, 99% purity) was purchased from FSA (England). The water in this work was Milli-Q ultrapure water.

Preparation and characterization of CaCO₃ nanoparticles

Synthesis of $CaCO_3$ nanoparticles was carried out using a colloidal gas aphron (CGA) generator similar to that described by the others [27-29]. Briefly, 212 mg (1mmol) of Na_2CO_3 and 200 mg of SDS were dissolved in 450 mL water as the mother solution for CGA preparation. Then 50 mL of a solution containing 147 mg (1mmol) of $CaCl_2.2H_2O$ was steadily injected to the prepared CGAs for 15 minutes. The precipitated particles from the totally collapsed foam were centrifuged (9000 rpm, 15 min) and rinsed several times with the copious amount of cold ethanol and distilled water for removing any residual surfactant. The detailed characterization results of the obtained nanoparticles were reported in our previous work [26].

Heavy metal ions adsorption experiments

Stock solutions of heavy metal ions (1000 mg/L) were prepared by dissolving the precise amount of $Pb(NO_3)_2$ and $FeSO_4.7H_2O$ in distilled water. These solutions were diluted to 10–200 mg/L for adsorption experiments. The initial pH of solutions was adjusted using diluted HNO_3 when needed. All the adsorption tests were performed batch-wise using a thermostatic shaker with controlled temperature and shaking speed (120 rpm). Briefly, 0.025-0.075 g of $CaCO_3$ was added to 50 ml of metal solution (10-200 mg/L) and shaken for 2 hours. The final concentrations of heavy metal ions in the samples were measured using atomic adsorption spectroscopy (VGP-210, Buck Scientific Inc). The adsorption capacity (q_e, mg/g) and removal efficiency (Re (%)) of heavy metal ions were calculated using the following equations:

$$q_e = \frac{(C_0 - C_e) \times V}{w} \tag{1}$$

$$Re(\%) = \frac{(C_0 - C_e)}{C_0} \times 100 \tag{2}$$

Where C_0 and C_e are the initial and equilibrium concentrations of solute (mg/L) in the solution, V is the solution volume (mL) and w is the mass of adsorbent (CaCO$_3$) (mg).

Design of experiments

The effects of temperature, heavy metal concentration, and adsorbent dosage on the removal capacity of CaCO$_3$ nanoparticles were evaluated by the response surface methodology (RSM) using DESIGN EXPERT 7.0.0 software (Stat-Ease Inc, Minneapolis, MN, USA). Optimum conditions were determined using a 3-level, 3-factor Box-Behnken Design (BBD). Table 1 represents the coded and uncoded ranges of selected parameters.

The adsorption capacity of calcium carbonate (Y) was expressed as a function of selected independent variables using a second order polynomial equation (Eq. 3).

$$Y = \beta_0 + \sum_{i=1}^{k} \beta_i X_i + \sum_{i=1}^{k} \beta_{ii} X_i^2 + \sum_{i=1}^{k} \sum_{j=1}^{k} \beta_{ij} X_i X_j + \varepsilon \quad (3)$$

Where Y is the predicted response, X_i and X_j ($i, j=1...k$) are independent parameters, β_0 is the intercept constant, β_i, β_{ii} and β_{ij} ($i, j=1...k$) are linear, square, and interactive coefficients respectively and ε is a random error.

RESULTS AND DISCUSSION

Characterization of CaCO$_3$

Physical properties of the adsorbent were reported elsewhere [26]. The produced particles had monosized vaterite polymorph with the main particle size of 100 nm and a surface area and average pore diameter of 76 m^2 g^{-1} and ~6.1 nm (SEM, XRD, and BET analysis).

Effects of pH and contact time

The removal percentage of CaCO$_3$ (1g/L) for Pb^{2+} and Fe^{2+} ions (200ppm) was evaluated in a pH range of 2.5-6 and not more than 6 for avoiding their precipitation (Fig. 1). It can be observed that the adsorption increases with an increase in pH, and reaches a plateau value at the pH range of 5.5-6. Lower pH decreases the removal efficiency of heavy metals due to an increase in solubility of each ion

in the solution. Moreover, lower pH values partially dissolve the calcium carbonate adsorbent particles. However, in pH values more than the precipitation limits of heavy metal ions in aqueous solutions, precipitation interferes with the adsorption process (pH>6). According to Fig. 1, the pH of 5.5 was selected for all the following experiments.

The kinetics of adsorption is shown in Fig. 2. The removal percentage of both metals on the adsorbent increases with contact time. It can be seen that at all the selected concentrations, more than 80% of the process was completed during the first hour and it achieves to equilibrium in the second hour. Therefore, a contact time of 2 hours was chosen for all the following experiments.

Adsorption kinetics

In order to investigate the mechanism of reactions, the kinetic parameters were evaluated using pseudo-first-order (PFO) [30] and pseudo-second-order (PSO) [31] kinetic models. The obtained data from Fig. 3 were utilized for this purpose. The linear forms of PFO and PSO equations can be expressed as:

$$ln\left(q_e - q_t\right) = \ln q_e - k_1 t \quad (4)$$

$$\frac{t}{q_t} = \frac{1}{k_2 q_e^2} + \frac{1}{q_e} t \quad (5)$$
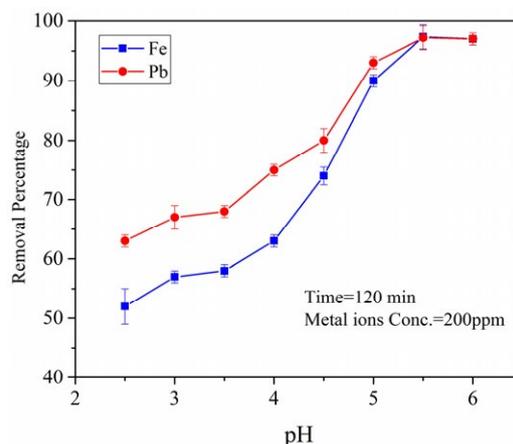

Fig. 1: Effect of pH on the adsorption of Pb^{2+} and Fe^{2+} ions.

Table 1: Experimental levels of independent parameters used in RSM design

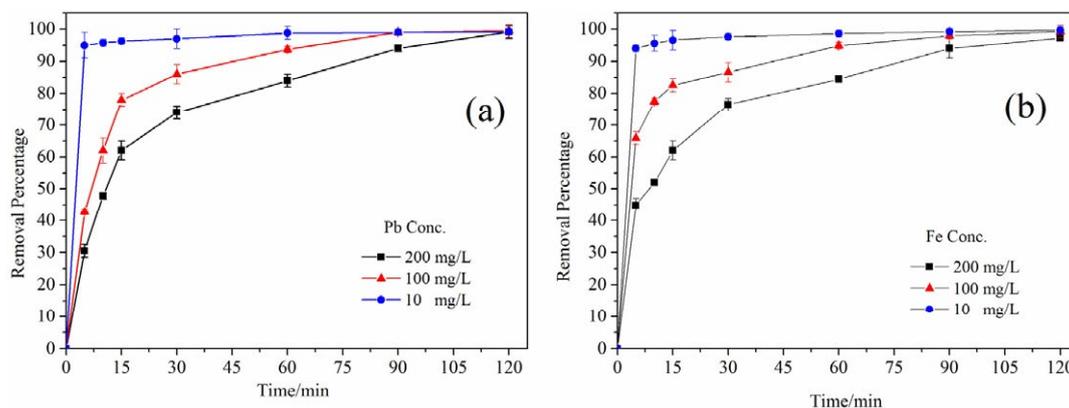| Variables	Factors	Range and level		
		-1	0	+1
Temperature, °C	X_1	25	45	65
CaCO$_3$ dosage, g/l	X_2	0.5	1	1.5
Initial metal concentration, ppm	X_3	10	105	200

Fig. 2: Kinetic adsorption of a) Pb^{2+} and b) Fe^{2+} on calcium carbonate nanoparticles, (pH= 5.5, T=25 ºC, adsorbent dosage =1 g/L).
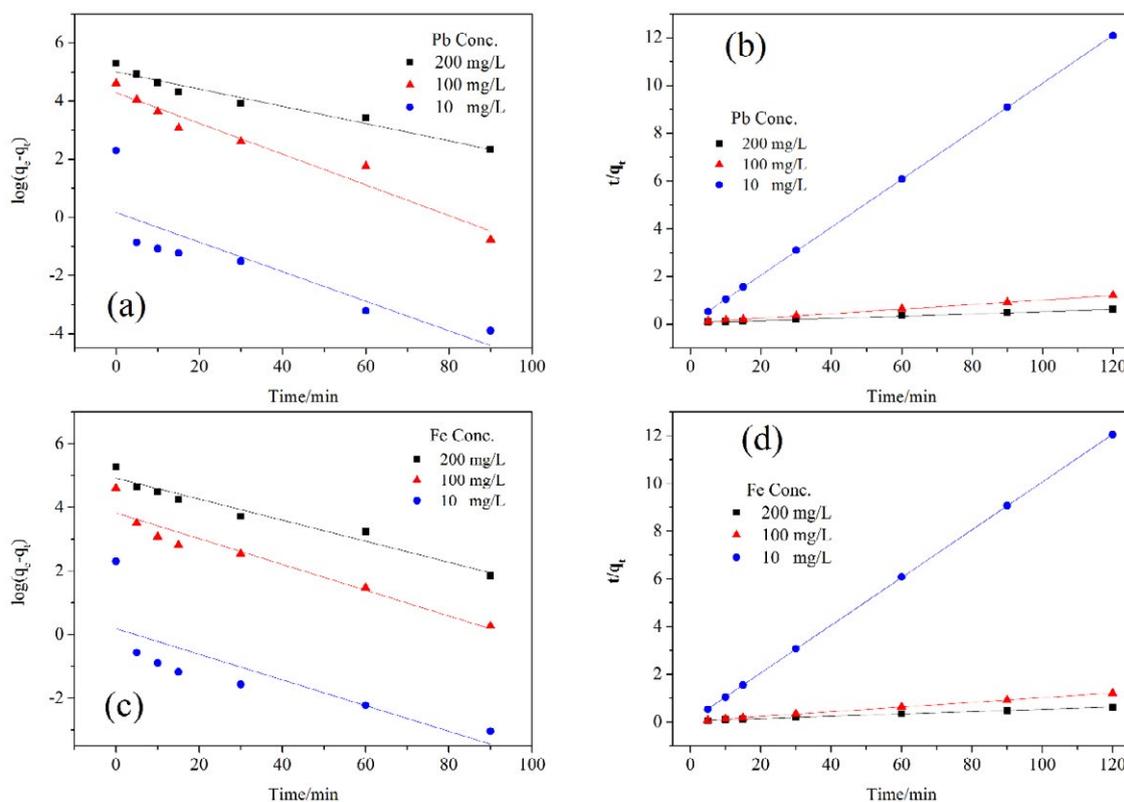

Fig. 3: The linearized pseudo-first-order kinetic (a, c) and pseudo-second-order kinetic (b, d) plots for adsorption of heavy metal ions onto $CaCO_3$ nanoparticles.

Where q_e and q_t are the sorption capacity (mg/g) at equilibrium and time t (min), and k_1 (min^{-1}) and k_2 (g/mg.min) are the rate constants of the PFO and PSO equations respectively.

The adsorption kinetic constants calculated based on the fitting results of PFO and PSO equations (Fig. 3) are summarized in Table 2. The higher R-squared values of the PSO model (R^2>0.99) compared with

the PFO model show that the experimental data were better described by this model.

Adsorption isotherms and effect of temperature

Fig. 4 demonstrates the adsorption isotherm of Pb^{2+} and Fe^{2+} adsorbed onto $CaCO_3$ nanoparticles over a wide range of initial concentration (10–4000 mg/L) and various temperatures. It can be seen that the

144

J. Water Environ. Nanotechnol., 3(2): 141-149 Spring 2018

equilibrium adsorption capacity of adsorbent increases at higher metal concentration. The maximum equilibrium uptake for Pb^{2+} ion (1210±30 mg/g) was noticeably more than Fe^{2+} ion (845±8 mg/g). However, no significant changes in the isotherms were observed with increasing the temperature.

Langmuir and Freundlich adsorption isotherms were used to analyze the mechanism of adsorbate–adsorbent interactions (Eqs. 6 and 7). The linear forms of Langmuir and Freundlich equations can be expressed as follow:

$$\frac{C_{eq}}{q_e} = \frac{1}{q_{max}K_{Lang}} + \frac{1}{q_{max}}C_{eq} \qquad (6)$$

$$\ln q_e = \ln K_{Freu} + \frac{1}{n}\ln C_{eq} \qquad (7)$$

Where C_{eq} is the equilibrium concentration of adsorbate ions in the solution (mg/L), q_{max} is the maximum adsorption uptake of metal ions at equilibrium (mg/g), and K_{Lang} (L/mg) and K_{Freu} (mg/g) are the Langmuir and Freundlich constants. The calculated Langmuir and Freundlich parameters are presented in Table 3. The R-squared values show that the experimental data are better fitted to Langmuir isotherm model ($R^2 > 0.99$). The values of Freundlich constants, K_{Freu} and n indicate the favorable adsorption of metal ions by $CaCO_3$ nanoparticles over the entire studied concentrations (n>1) [32].

The extraordinary amounts calculated for the maximum adsorption uptake obtained from the Langmuir isotherm were in good agreement with

Table 2: The kinetic constants for the adsorption of metal ions on $CaCO_3$ nanopaticles

Initial metal Conc., ppm		q_e, experimental	Pseudo-first-order equation			Pseudo-second-order equation		
			k_1 (min^{-1})	$q_{e,\,model}$	R^2	k_2 (g/mg.min)	$q_{e,\,model}$	R^2
Pb	10	9.92	0.05	1.18	0.726	0.222	10	1
	100	99.45	0.078	52.09	0.95	1.29×10^{-3}	111.11	0.999
	200	198.2	0.027	133.35	0.974	2.67×10^{-4}	250	0.997
Fe	10	9.97	0.04	1.2	0.623	0.189	10	0.998
	100	99.26	0.04	45.83	0.959	2.25×10^{-3}	109.11	0.997
	200	194.4	0.033	136.87	0.923	3.48×10^{-4}	251	0.996

Table 3: Adsorption isotherm parameters for Pb^{2+} and Fe^{2+} ions using calcium carbonate nanoparticles at different temperatures

Temp. (K)		Langmuir constants			Freundlich constants		
		q_{max} (mg/g)	K_{Lang} (l/mg)	R^2	K_{Freu} (mg/g)	n	R^2
Pb	298	1237.01	0.0517	0.9999	64.71	1.86	0.5534
	318	1243.06	0.06	0.9998	75.04	1.96	0.522
	338	1291.01	0.0561	0.9997	80.79	2.21	0.7428
Fe	298	854.7	0.0323	0.998	62.17	2.56	0.9157
	318	862	0.0246	0.996	57.32	2.5	0.9081
	338	862.07	0.0358	0.998	71.19	2.66	0.8719
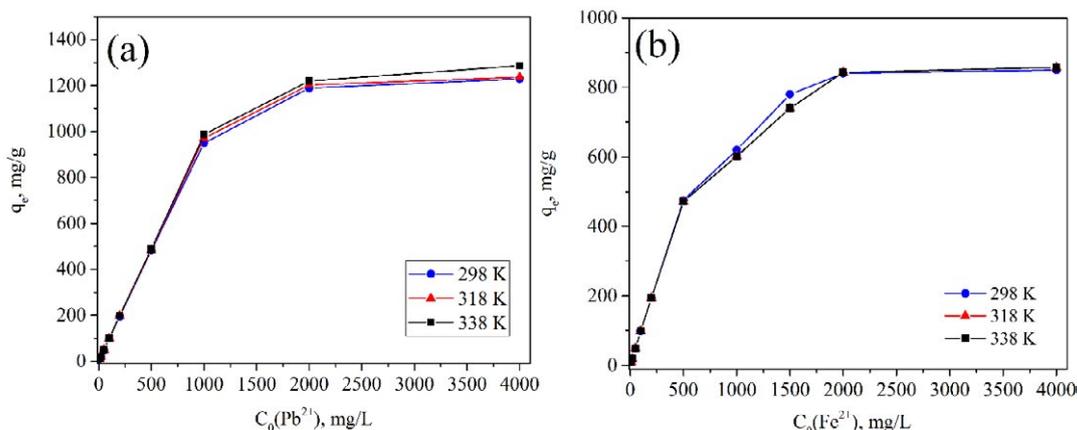
Fig. 4: Adsorption isotherms of $CaCO_3$ nanoparticles for (a) Pb^{2+} and (b) Fe^{2+} at different temperatures.

J. Water Environ. Nanotechnol., 3(2): 141-149 Spring 2018

145

similar studies [24, 25]. Ma *et al.* and Cai *et al.* mentioned that the $CaCO_3$ adsorption mechanism is not just a simple monolayer adsorption and transformation of precipitation between $CaCO_3$ and heavy metal carbonates could be the explanation for the large adsorption capacity of $CaCO_3$. However, natural types of calcium carbonate adsorbents employed in some studies did not show such great adsorption uptakes [33-36]. For instance; the maximum adsorption uptake reported for lead, varies from 0.0167 mg/g to 3242.48 mg/g using limestone [34] and hierarchical $CaCO_3$–maltose meso/macroporous hybrid materials [25], respectively. We found that the size and crystal structure of calcium carbonate are important to improve the transformation of precipitation between $CaCO_3$ and heavy metal carbonates. Calcite is the most thermodynamically stable polymorph of calcium carbonate in nature and has a lower solubility in comparison with other polymorphs of calcium carbonate like vaterite and amorphous calcium carbonate (ACC) [37]. Moreover, nanosized particles may also show higher solubility in aqueous solutions rather than large ones [38]. Therefore, nanosized and more soluble polymorphs of $CaCO_3$ used by Ma *et al.* and Cai *et al.* may have facilitated the adsorption mechanism proposed by them [24, 25]. The large adsorption capacity of vaterite nanoparticles observed in this study could be the result of a similar transformation of precipitation between $CaCO_3$ and heavy metal carbonates.

Analysis of Experimental Data

The effects of temperature, adsorbent dosage, and heavy metal initial concentration were evaluated by using an experimental procedure based on Box-Behnken design with five center point replicates, which resulted in 17 experimental runs (Table 4).

According to the RSM results, quadratic model equations were employed to express the association

Table 4: Experimental design and experimental/predicted responses for Pb^{2+} and Fe^{2+} removal

Run No.	Temp (°C)	$CaCO_3$ Dosage (g/L)	Metal initial Conc. (mg/L)	Adsorption capacity (mg/g)			
				Pb^{2+}		Fe^{2+}	
				Experimental	Predicted	Experimental	Predicted
1	25	1	200	194.7	211.17	194.4	209.70
2	65	0.5	105	205.73	204.50	209.06	207.90
3	65	1	200	198.5	214.63	197	212.00
4	25	0.5	105	204.2	202.63	207.9	206.44
5	45	1.5	200	140	122.31	129.8	113.34
6	65	1	10	9.91	6.56	9.94	5.36
7	45	0.5	10	19.64	37.33	17.32	33.78
8	45	1	105	102.2	101.82	103.9	103.84
9	45	1	105	102	101.82	104	103.84
10	25	1	10	9.82	6.31	9.98	5.01
11	45	1	105	100.5	101.82	103.9	103.84
12	45	1.5	10	7.71	22.61	6.45	20.29
13	45	1	105	101.5	101.82	103.8	103.84
14	25	1.5	105	67.32	68.54	69.3	70.46
15	45	0.5	200	391.2	376.30	386.64	372.80
16	45	1	105	102.92	101.82	103.6	103.84
17	65	1.5	105	68.31	69.88	69.5	70.96

Table 5: Analysis of variance (ANOVA) results on the quadratic model for metal removal from aqueous solution

Factors	Pb (R^2=0.9682)		Fe (R^2=0.9723)	
	Fisher's F-test	p-value	Fisher's F-test	p-value
Model	55.15	<0.0001	63.29	<0.0001
X_1	0.017	0.9006	0.007	0.9345
X_2	117.88	<0.0001	140.94	<0.0001
X_3	314.13	<0.0001	353.19	<0.0001
X_1X_2	2.38×10^{-4}	0.9881	8.7×10^{-4}	0.9773
X_1X_3	0.011	0.9186	6.6×10^{-3}	0.9374
X_2X_3	46.73	0.0002	57.23	0.0001
X_1^2	0.012	0.9172	0.033	0.861
X_2^2	17.31	0.0042	18.05	0.0038
X_3^2	0.075	0.7928	0.095	0.7663

between the response and independent variables (Eqs 8 and 9). The insignificant variables are excluded in these equations.

$$Y = 122.77 - 285.4X_2 + 2.34X_3 \cdot$$
$$+141.94X_2^2 - 1.26X_2X_3 \tag{8}$$

$$Y = 123.39 - 286.84X_2 + 2.47X_3 \cdot$$
$$+134.64X_2^2 - 1.29X_2X_3 \tag{9}$$

Interactions among the independent variables and obtained responses were analyzed using the analysis of variance (ANOVA) (Table 5). Results
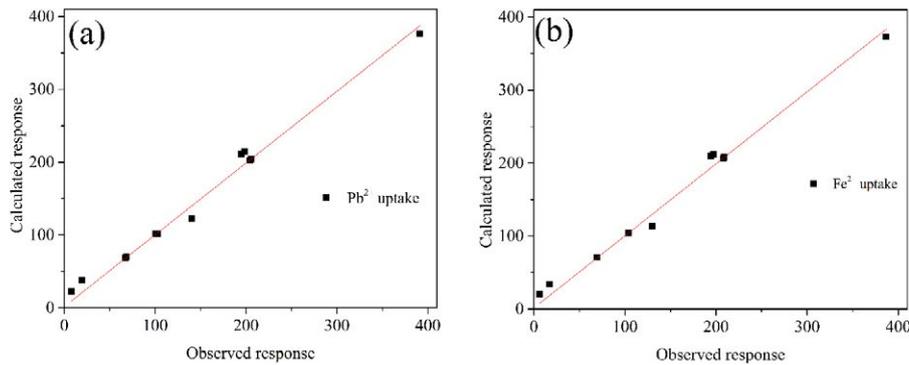

Fig. 5: Comparison of experimental and calculated responses for (a) Pb^{2+} and (b) Fe^{2+} metal ions removal.
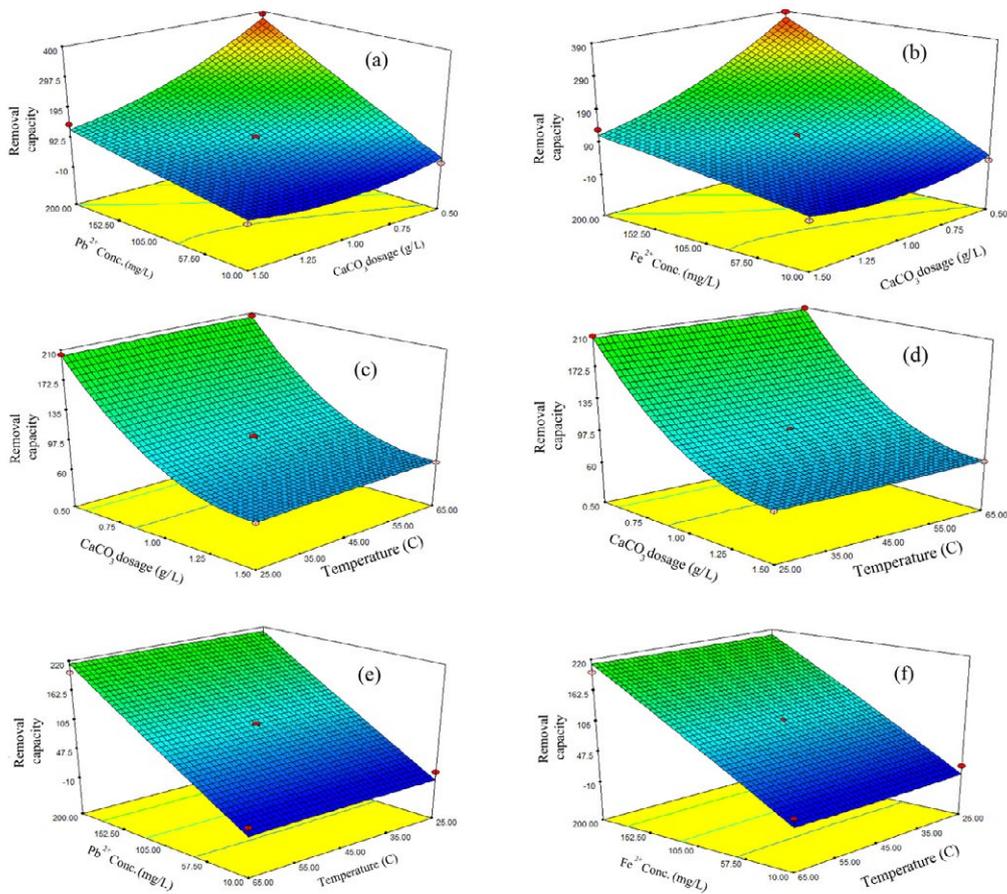

Fig. 6: 3D response surface diagrams showing the effects of mutual interactions between two independent variables.

of the Fisher's F-test with a low probability (P-value<0.0001) confirm that both models are highly significant. The F-values of different independent variables indicate that the only significant model terms are X_2, X_3, X_2X_3, and X_2^2 (p-value<0.05). The fit quality of the models was further evaluated by the R^2 value. The R^2 values for Pb^{2+} and Fe^{2+} removal models were 0.9682 and 0.9723 respectively. This indicates that there is a good agreement between the experimental and predicted values. The adequacy of regression models with the experimental data is also graphically shown in Fig. 5.

Three-dimensional (3D) response surface and the corresponding contour plots were utilized to assess the interaction between two significant independent variables and their effects on the response (Fig. 6). Fig. 6 (a and b) shows that the removal uptake was increased with increasing heavy metal concentration and decreasing $CaCO_3$ dosage. According to Fig. 6 (c-f), the temperature was found to be insignificant on the response for both Pb^{2+} and Fe^{2+} removal uptakes. The optimum values for maximizing the removal capacity of $CaCO_3$ were also obtained using Design-Expert 7.0.0 software. The optimized parameters suggested by the software for temperature, $CaCO_3$ dosage, and metal concentration were 65 °C, 0.5 g/L and 200 mg/L for both Pb^{2+} and Fe^{2+} ions which were in good agreement with the experimental data.

CONCLUSIONS

Removal of Pb and Fe ions from aqueous solutions by calcium carbonate adsorbent was examined in batch-wise experiments. It was found that the maximum observed adsorption capacities of particles were 1210±30 mg/g for Pb(II) and 845±8 mg/g for Fe(II), at 25°C and pH=5.5. Analyzing the experimental data by kinetic and thermodynamic models revealed that the high removal capacity of the nano adsorbent is not just because of a simple monolayer adsorption process but it could be the result of a transformation/ precipitation mechanism between the $CaCO_3$ and heavy metal carbonates. The most important parameters were found to be adsorbent dosage and heavy metal concentration respectively. The effect of temperature was found to be negligible within the experimental range.

ACKNOWLEDGMENT

CONFLICT OF INTEREST

The authors declare that there are no conflicts of interest regarding the publication of this manuscript.

REFERENCES

1. Paulino AT, Minasse FAS, Guilherme MR, Reis AV, Muniz EC, Nozaki J. Novel adsorbent based on silkworm chrysalides for removal of heavy metals from wastewaters. Journal of Colloid and Interface Science. 2006;301(2):479-87.
2. Gupta VK, Agarwal S, Saleh TA. Synthesis and characterization of alumina-coated carbon nanotubes and their application for lead removal. Journal of Hazardous Materials. 2011;185(1):17-23.
3. Zhang F-S, Nriagu JO, Itoh H. Mercury removal from water using activated carbons derived from organic sewage sludge. Water Research. 2005;39(2-3):389-95.
4. Boparai HK, Joseph M, O'Carroll DM. Kinetics and thermodynamics of cadmium ion removal by adsorption onto nano zerovalent iron particles. Journal of Hazardous Materials. 2011;186(1):458-65.
5. Argun ME. Use of clinoptilolite for the removal of nickel ions from water: Kinetics and thermodynamics. Journal of Hazardous Materials. 2008;150(3):587-95.
6. Fu F, Xie L, Tang B, Wang Q, Jiang S. Application of a novel strategy—Advanced Fenton-chemical precipitation to the treatment of strong stability chelated heavy metal containing wastewater. Chemical Engineering Journal. 2012;189-190:283-7.
7. Stojanovic A, Keppler BK. Ionic Liquids as Extracting Agents for Heavy Metals. Separation Science and Technology. 2012;47(2):189-203.
8. Naushad M, Mittal A, Rathore M, Gupta V. Ion-exchange kinetic studies for Cd(II), Co(II), Cu(II), and Pb(II) metal ions over a composite cation exchanger. Desalination and Water Treatment. 2014;54(10):2883-90.
9. Al-Zoubi H, Ibrahim KA, Abu-Sbeih KA. Removal of heavy metals from wastewater by economical polymeric collectors using dissolved air flotation process. Journal of Water Process Engineering. 2015;8:19-27.
10. Cui Y, Ge Q, Liu X-Y, Chung T-S. Novel forward osmosis process to effectively remove heavy metal ions. Journal of Membrane Science. 2014;467:188-94.
11. Khan NA, Hasan Z, Jhung SH. Adsorptive removal of hazardous materials using metal-organic frameworks (MOFs): A review. Journal of Hazardous Materials. 2013;244-245:444-56.
12. Skubal LR, Meshkov NK, Rajh T, Thurnauer M. Cadmium removal from water using thiolactic acid-modified titanium dioxide nanoparticles. Journal of Photochemistry and Photobiology A: Chemistry. 2002;148(1-3):393-7.
13. Fu F, Wang Q. Removal of heavy metal ions from wastewaters: A review. Journal of Environmental Management. 2011;92(3):407-18.
14. Lo S-F, Wang S-Y, Tsai M-J, Lin L-D. Adsorption capacity and removal efficiency of heavy metal ions by Moso and

Ma bamboo activated carbons. Chemical Engineering Research and Design. 2012;90(9):1397-406.

15. Al-Othman ZA, Ali R, Naushad M. Hexavalent chromium removal from aqueous medium by activated carbon prepared from peanut shell: Adsorption kinetics, equilibrium and thermodynamic studies. Chemical Engineering Journal. 2012;184:238-47.

16. Hegazy EZ, Abdelmaksod IH, Kosa SA. Removal of Heavy Metal Quaternary Cations Systems on Zeolite A and X Mixtures Prepared from Local Kaolin. CLEAN - Soil, Air, Water. 2013;42(6):775-8.

17. Wen J, Yi Y, Zeng G. Effects of modified zeolite on the removal and stabilization of heavy metals in contaminated lake sediment using BCR sequential extraction. Journal of Environmental Management. 2016;178:63-9.

18. Sud D, Mahajan G, Kaur M. Agricultural waste material as potential adsorbent for sequestering heavy metal ions from aqueous solutions – A review. Bioresource Technology. 2008;99(14):6017-27.

19. Miretzky P, Cirelli AF. Hg(II) removal from water by chitosan and chitosan derivatives: A review. Journal of Hazardous Materials. 2009;167(1-3):10-23.

20. Gupta VK, Nayak A. Cadmium removal and recovery from aqueous solutions by novel adsorbents prepared from orange peel and Fe2O3 nanoparticles. Chemical Engineering Journal. 2012;180:81-90.

21. Liu J-f, Zhao Z-s, Jiang G-b. Coating Fe3O4Magnetic Nanoparticles with Humic Acid for High Efficient Removal of Heavy Metals in Water. Environmental Science & Technology. 2008;42(18):6949-54.

22. Charpentier TVJ, Neville A, Lanigan JL, Barker R, Smith MJ, Richardson T. Preparation of Magnetic Carboxymethylchitosan Nanoparticles for Adsorption of Heavy Metal Ions. ACS Omega. 2016;1(1):77-83.

23. Kandah MI, Meunier J-L. Removal of nickel ions from water by multi-walled carbon nanotubes. Journal of Hazardous Materials. 2007;146(1-2):283-8.

24. Cai G-B, Zhao G-X, Wang X-K, Yu S-H. Synthesis of Polyacrylic Acid Stabilized Amorphous Calcium Carbonate Nanoparticles and Their Application for Removal of Toxic Heavy Metal Ions in Water. The Journal of Physical Chemistry C. 2010;114(30):12948-54.

25. Ma X, Li L, Yang L, Su C, Wang K, Yuan S, *et al*. Adsorption of heavy metal ions using hierarchical CaCO3–maltose meso/macroporous hybrid materials: Adsorption isotherms and kinetic studies. Journal of Hazardous Materials. 2012;209-210:467-77.

26. Mohammadifard H, Banifatemi SS, Amiri MC. Growing Innovative Calcium Carbonate Morphologies by Utilizing the Colloidal Gas Aphron System as a Surfactant-Based Template Method. Chemical Engineering Communications. 2016;203(9):1165-72.

27. Stephan W. Foams and biliquid foams-aphrons. Chister, New York, Brisbane, Toronto, Singapore: John Wiley & Sons, 1987, 236 S., ? 29.50, ISBN 0-471-91685-4. Acta Biotechnologica. 1989;9(1):68-.

28. Amiri MC, Sadeghialiabadi H. Evaluating the stability of colloidal gas aphrons in the presence of montmorillonite nanoparticles. Colloids and Surfaces A: Physicochemical and Engineering Aspects. 2014;457:212-9.

29. Amiri M. Effect of gas transfer on separation of whey protein with aphron flotation. Separation and Purification Technology. 2004;35(2):161-7.

30. Yuh-Shan H. Citation review of Lagergren kinetic rate equation on adsorption reactions. Scientometrics. 2004;59(1):171-7.

31. Ho Y. Review of second-order models for adsorption systems. Journal of Hazardous Materials. 2006;136(3):681-9.

32. Frimmel FH, Huber L. Influence of humic substances on the aquatic adsorption of heavy metals on defined mineral phases. Environment International. 1996;22(5):507-17.

33. Ziyadanoğullari B, Yavuz Ö, Aydin F, Aydin I, Bingöl H. Removal of cadmium from aqueous solution by a soil containing magnesite. Archives of Agronomy and Soil Science. 2004;50(4-5):371-6.

34. Aziz HA, Adlan MN, Ariffin KS. Heavy metals (Cd, Pb, Zn, Ni, Cu and Cr(III)) removal from water in Malaysia: Post treatment by high quality limestone. Bioresource Technology. 2008;99(6):1578-83.

35. Al-Degs YS, El-Barghouthi MI, Issa AA, Khraisheh MA, Walker GM. Sorption of Zn(II), Pb(II), and Co(II) using natural sorbents: Equilibrium and kinetic studies. Water Research. 2006;40(14):2645-58.

36. Ahmad M, Usman ARA, Lee SS, Kim S-C, Joo J-H, Yang JE, *et al*. Eggshell and coral wastes as low cost sorbents for the removal of Pb2+, Cd2+ and Cu2+ from aqueous solutions. Journal of Industrial and Engineering Chemistry. 2012;18(1):198-204.

37. De Visscher A, Vanderdeelen J. Estimation of the Solubility Constant of Calcite, Aragonite, and Vaterite at 25ºC Based on Primary Data Using the Pitzer Ion Interaction Approach. Monatshefte fur Chemie / Chemical Monthly. 2003;134(5):769-75.

38. Adamson A. W., and Gast A. P., 1997.Physical Chemistry of Surfaces, New York: John Wiley & Sons.

J. Water Environ. Nanotechnol., 3(2): 141-149 Spring 2018

149